Available online at www.sciencedirect.com
SCIENCE DIRECT®
International Journal of Mass Spectrometry 231 (2004) 59–68
International Journal of Mass Spectrometry
www.elsevier.com/locate/ijms

Climbing the internal energy ladder: the unimolecular decomposition of ionized poly(vinyl acetate)

Marie-Soleil Giguère, Paul M. Mayer*

Chemistry Department, University of Ottawa, 10 Marie-Curie, Ottawa, Ont., Canada K1N 6N5

Received 8 July 2003; accepted 15 September 2003

Abstract

The dissociation of gas-phase poly(vinyl acetate) ionized by Li^+ was investigated by electrospray-ionization tandem mass spectrometry. The ions lose acetic acid molecules from the polymer side chain, and ultimately lithium acetate, to form a polyene with a positive charge on the carbon backbone. Collision-induced dissociation (CID) mass spectra were obtained at different center-of-mass collision energies to study the sequential appearance of the fragment ions. Molecular mechanics/molecular dynamics (MM/MD), semi-empirical, Hartree–Fock and density functional calculations were employed to model the lowest energy dissociation processes.

Keywords: Electrospray-ionization mass spectrometry; Poly(vinyl acetate); CID; MM/MD; Ab initio calculations; Density functional theory; Unimolecular decomposition

1. Introduction

Collision-induced dissociation (CID) mass spectrometry permits the primary structure (sequence) of an ionized polymer to be determined. The fragmentation patterns exhibited by many polymer ions have been attributed to backbone cleavage along the polymer chain. Jackson and co-workers [1–5] studied the fragmentation of poly(methyl methacrylate) (PMMA) ions generated by matrix-assisted laser desorption/ionization (maldi) under conditions of high-energy collision-induced dissociation. Two main progressions of distonic ion fragments were observed that are formed by homolytic cleavage of the tertiary C–C bonds along the polymer backbone starting from each end of the polymer (Scheme 1). The resulting ion *m*/*z* value depends on which fragment retains the metal cation. Minor products due to 1,5-hydrogen rearrangement reactions were also observed to occur from both ends of the polymer. Molecular modeling of the gas-phase structure of PMMA ionized with Na^+ showed that the oligomers adopt a closed-loop shape with the ester side chains of the polymer complexing the metal cation [5]. The same group studied the fragmentation of ionized poly(styrene) (PS) [4,6–8] and its gas-phase conformation [9]. Closely related mechanisms have been proposed for its fragmentation. The gas-phase structure of the PS ion shows coordination of the metal by the phenyl ring on the side chain of the polymer. Unlike ionized PMMA, the structure of ionized PS is close to linear; the metal cation lies between two phenyl rings in the middle of the polymer backbone.

This trend in fragmentation along the polymer backbone extends to more polar polymers such as poly(3-hydroxybutanoic acid) ionized with a potassium or sodium cation [10] and polyols such as poly(ethylene oxide) and poly(propylene oxide) ionized with silver [11]. Selby et al. [12] have shown that low-energy CID of poly(ethylene glycol) (PEG) ionized with an alkali metal cation yields metal cations and small fragments from hydrogen-rearrangement reactions. At higher collision energies, 1,4-H_2 eliminations are observed producing two types of unsaturated fragment ions along with homolytic cleavage reactions at either end the polymer. Derrick and co-workers [13] and Jackson et al. [4] also observed the presence of these three types of products. Gidden et al. [14] modeled the gas-phase conformation of ionized PEG and poly(propylene glycol) (PPG) and as observed for PMMA the polymer surrounds the metal allowing the oxygen atoms on the backbone to coordinate the cation.

* Corresponding author. Tel.: +1-613-562-5800x6038; fax: +1-613-562-5170.
E-mail address: pmayer@science.uottawa.ca (P.M. Mayer).

1387-3806/$ – see front matter © 2003 Elsevier B.V. All rights reserved.
doi:10.1016/j.ijms.2003.09.013

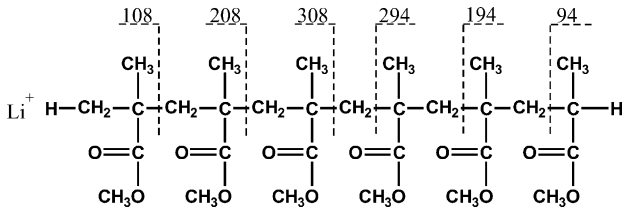

Scheme 1. CID fragmentation pattern of poly(methyl methacrylate) Li.

In this study the fragmentation of ionized poly(vinyl acetate) (PVAc) generated by ESI-MS and ESI-MS/MS has been modeled to understand the mechanism of dissociation and the internal energy effects on the CID processes. Vinyl acetate is a monomer used for the fabrication of adhesives and sealants related to the paper, textile and wood industries.

2. Experimental procedures

2.1. Polymer synthesis

Poly(vinyl acetate) was produce by free radical polymerization. Vinyl acetate (Aldrich) was purified by distillation under vacuum. The initiator, azodiisobutyronitrile (AIBN), was recrystallized three times in methanol. The chain transfer agent dodecanethiol (Aldrich) and the solvent toluene (BDH Ltd.) were used without further purification. A reaction mixture containing about 17% (w/w) of monomer was pipetted into glass ampoules. After four freeze-pump-thaw cycles under vacuum to remove air, the ampoules were sealed and heated at 60 °C. Polymerization was stopped by transferring the ampoules to an ice bath. Solvent was evaporated and the resulting polymer samples were dissolved in acetone for analysis by ESI-MS. Oligomers of molecular weight between 400 and 2000 Da were produced. The reaction conditions were adjusted to achieve the desired molecular weight using a JAVA^{TM}-based program for simulation of free-radical polymerization developed by Badeen and Dubé [15].

2.2. Mass spectrometry

The ESI-MS and ESI-MS/MS experiments were performed using a Micromass Quattro LC triple quadrupole mass spectrometer equipped with a Z-spray source. Solutions of 1 mg/ml of polymer sample and 0.25 mg/ml of NaCl or LiCl in 9:1 acetone:water mixture were analyzed. The ESI capillary was operated at 4.3 kV and the sample cone voltage was 180 V. CID of the polymer ions utilized collision energies from 10 to 50 eV and argon was used as collision gas with pressures from 4×10^{-4} to 1.2×10^{-3} mbar. A flow rate of 60 μl/min of 9:1 acetone:water was used for MS and MS/MS analysis.

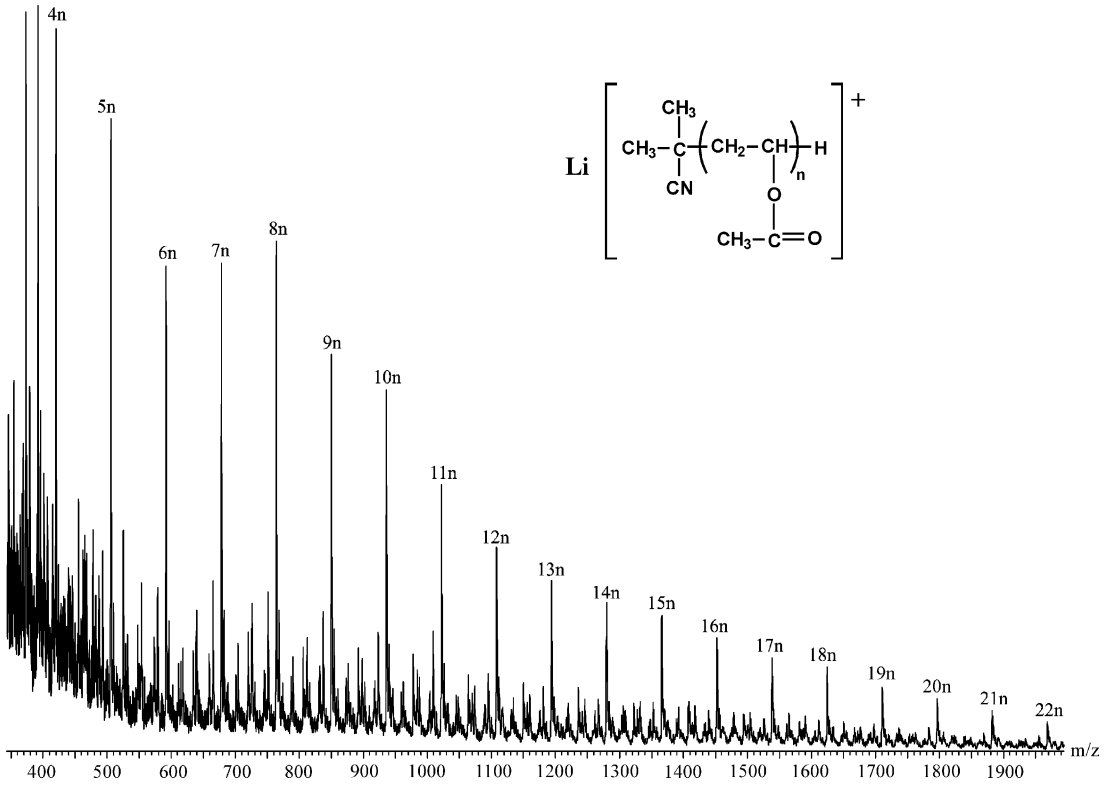

Fig. 1. ESI mass spectrum of the PVAc mixture ionized with lithium. One polymer distribution is observed ($Li^+ + 69 + 86n$) indicating that the end groups are hydrogen and isobutyronitrile.

2.3. Computational procedures

Molecular mechanics/molecular dynamics (MM/MD), semi-empirical, ab initio and density functional theory calculations were performed to predict the structure and the relative energies of poly(vinyl acetate) ions in the gas-phase and those of the fragmentation products observed by collision-induced dissociation mass spectrometry. The Cerius2 modeling environment [16] was used to model structures of a 5-mer of PVAc ionized with lithium and the experimentally observed fragments. To study the conformation of the polymer, equilibration and annealing dynamics were performed. During the equilibration phase an energy-minimized structure of the ionized polymer was run for 100 ps at constant NVT (constant number of moles, volume and temperature: 300 K) to determine the equilibrium structure. The lowest energy equilibrium structure was then evaluated at constant NVT using 100–200 annealing cycles in which the temperature was varied from 300 to 800 K in increments of 100 K. One thousand steps (1 ps) of dynamics were done at each temperature increment and the model was minimized to 0 K after each complete annealing cycle. Annealing cycles were continued until the energy of the structures reached a low energy plateau.

Standard ab initio molecular orbital calculations were done using the GAUSSIAN 98 [17] suite of programs. The geometries of the lowest energy conformations from the annealing runs for each species were optimized using semi-empirical (AM1) and density functional theory (B3-LYP/3-21G). The optimized geometries from each level of theory were used to calculate the single-point energy by Hartree–Fock and density functional theory (using the HF/6-31+G(d) and B3-LYP/6-31+G(d) levels of theory). All relative energies were corrected for zero-point vibrational energy (ZPVE) using the scaled (by 0.98 [18]) B3-LYP/3-21G values. The ZPVE values from semi-empirical theory were close to the DFT values (less than 5 kJ/mol of difference) but the B3-LYP values were chosen for consistency.

The transition state for the loss of acetic acid was modeled using a 3-mer of PVAc ionized with lithium. The geometry was optimized and the harmonic vibrational frequencies were calculated at the HF/6-31+G(d) level of theory. The IRC algorithm in GAUSSIAN 98 was used to verify all transition state structures.

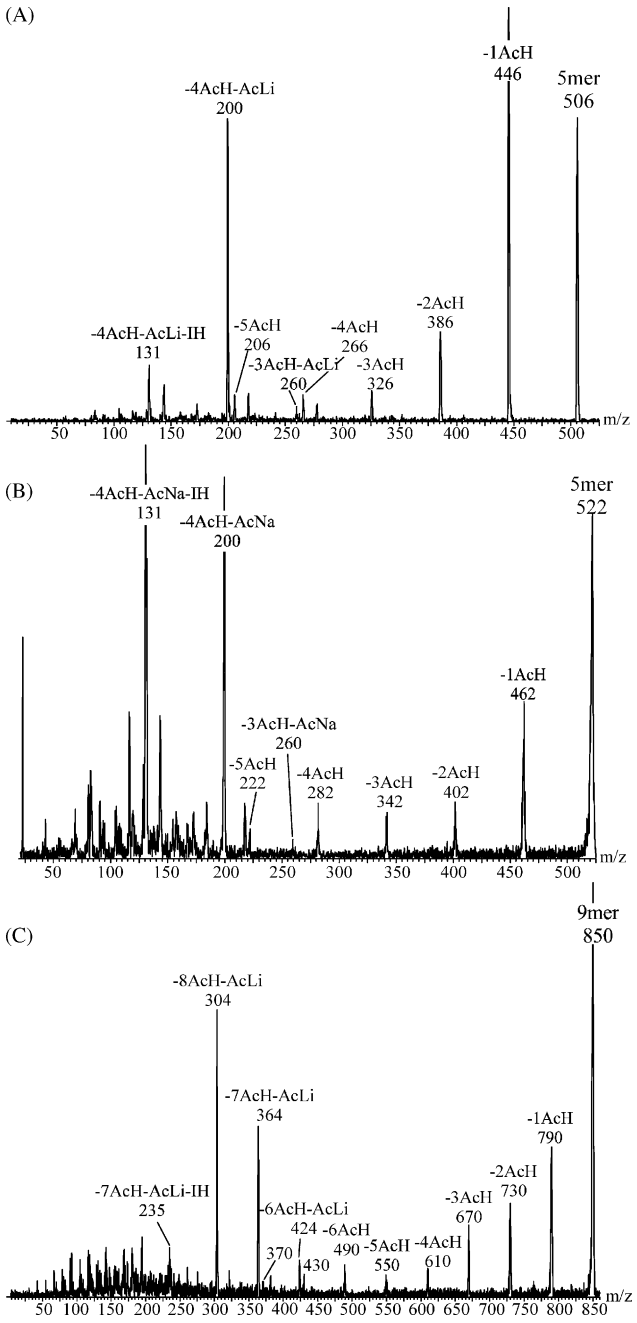

Fig. 2. CID mass spectrum of (A) $[PVAc_5 + Li]^+$, (B) $[PVAc_5 + Na]^+$, (C) $[PVAc_9 + Li]^+$. AcH: acetic acid, AcLi: lithium acetate, IH: isobutyronitrile. Lab frame collision energy = 26 eV.

3. Results and discussion

3.1. Mass spectrometry

Fig. 1 shows the ESI mass spectrum of the PVAc mixture ionized with lithium. One polymer distribution is observed ($Li^+ + 69 + 86n$) indicating that the end groups are hydrogen and isobutyronitrile (from the initiator of the polymerization). The peaks are separate by 86 mass units confirming that the repetition unit is vinyl acetate.

CID mass spectrometry was carried out on the 4-mer to the 12-mer using either sodium or lithium to ionize the polymer. The CID mass spectrum of $[PVAc_5 + Li]^+$ is shown in Fig. 2A. The mass spectrum shows acetic acid (AcH) loss from the polymer side chain. For the 5-mer, five repetitive losses are observed as well as two losses of lithium acetate (AcLi) (*m*/*z* 260 and 200). The peak at *m*/*z* 200 corresponds to a polyene chain with hydrogen and isobutyronitrile as end groups. The oligomer can then lose the initiator terminus resulting in a fragment ion appearing at *m*/*z* 131. The

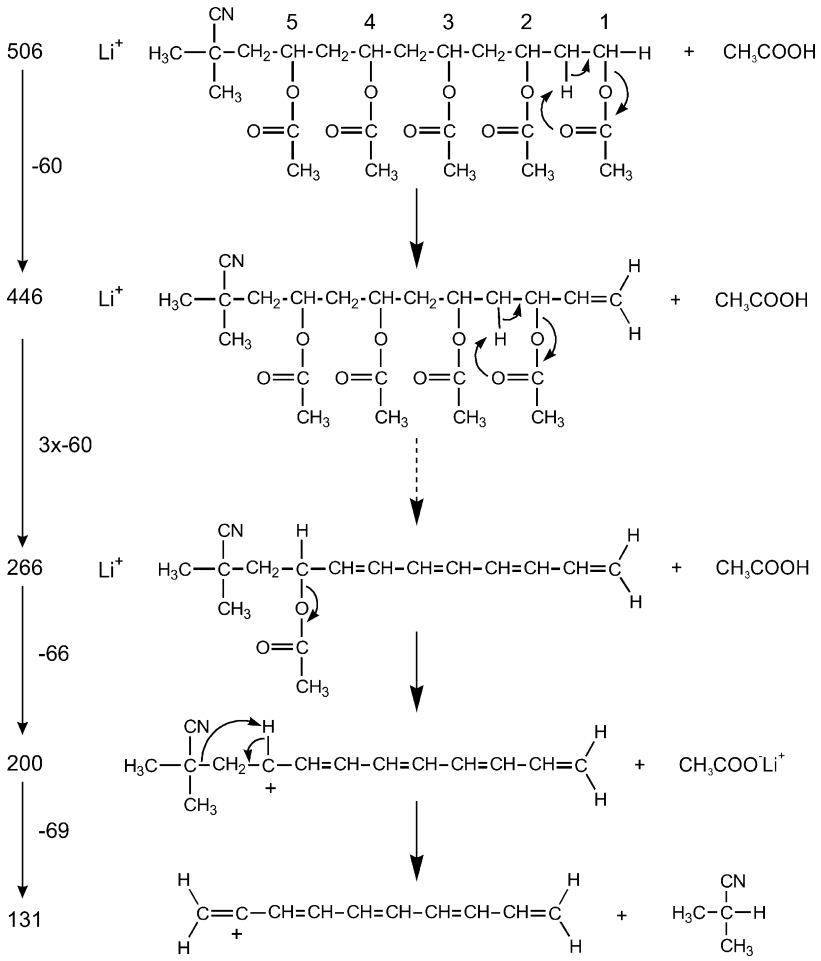

Scheme 2. Proposed fragmentation pathway for $[VAc_5 + Li]^+$.

fragment ions at *m*/*z* 260, 200, and 131 do not contain a metal cation since when the salt is change from LiCl to NaCl, the mass of these ions do not shift (Fig. 2B) while the other peaks are shifted in *m*/*z* by the difference in mass between ^{7}Li and ^{23}Na. Therefore, *m*/*z* 260, 200, and 131 have a positive charge on the polymer backbone. The fragmentation of $[PVAc_5 + Li]^+$ is summarized in Scheme 2. In the case of larger oligomers, most of the side chains are lost as acetic acids. The ion $[PVAc_9 + Li]^+$ (Fig. 2C) loses eight acetic acid molecules and there are three dissociation paths leading to the loss of lithium acetate. The polyene chains with and without the initiator end groups are at *m*/*z* 304 and 235, respectively.

The unlabeled peaks in the low mass range of each spectrum in Fig. 2 are independent of the salt used meaning they come from the fragmentation of the polyene chains. Pseudo MS^3 experiments on *m*/*z* 131 (resulting from skimmer-cone dissociation) showed peaks separated by 26 mass units consistent with the fragmentation of a carbocation chain with alternating single and double bonds.

The loss of a metal ion has been observed for poly(ethylene terephthalate) [4]. According to Jackson et al. [4], the loss of the metal ion was caused by the rigidity of the polymer resulting in weaker interactions between the heteroatoms of the polymer and the metal cation. In addition, fragment ions appearing at low *m*/*z* value in the CID mass spectrum of poly(styrene) are not metal ion adducts [3,7,8]. These peaks were more intense when a larger metal such as ^{107}Ag or ^{63}Cu was used to ionize the polymer. It was proposed that fragment ions with lower *m*/*z* ratio are less stable because of the weaker binding affinity with the metal ion. These hypotheses cannot be extended to PVAc where, as shown in Fig. 2C, the 9-mer produced large oligomeric fragments without metal ion adducts (*m*/*z* 304, 364, and 424).

A study of the relative abundance of the fragment ions versus collision energy was made at different collision gas pressures (4, 8 and 12×10^{-4} mbar) and is shown in Fig. 3 for the $[PVAc_5 + Li]^+$ ion at 8×10^{-4} mbar. The most abundant process (up to 2.2 eV) is the loss of one acetic acid to produce the peak with *m*/*z* 446. The second major fragment at *m*/*z* 200 corresponds to the loss of four acetic acid molecules and a metal acetate. This signal becomes dominant at a center-of-mass collision energy of 2.2 eV when the collision gas pressure is 8×10^{-4} mbar. This fragment appears before the emergence of peaks from multiple losses of acetic acid. The next dominant peak is the polyene

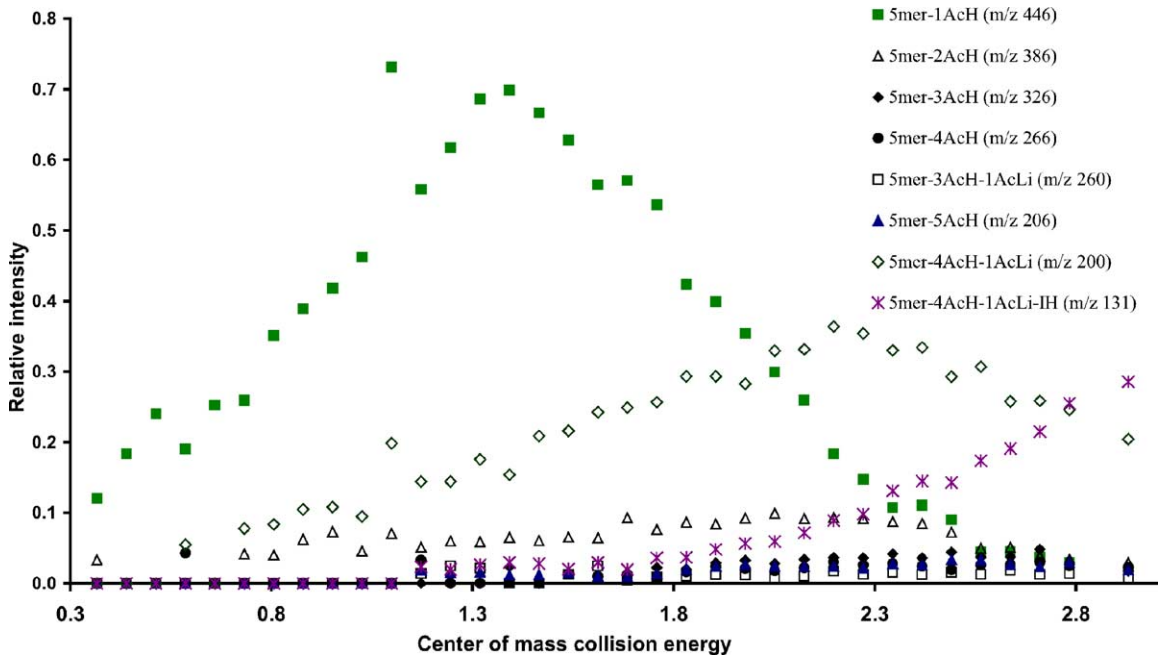

Fig. 3. CID mass spectrum of $[PVAc_5 + Li]^+$ at a collision gas pressure of 8×10^{-4} mbar as a function of collision energy. AcH: acetic acid, AcLi: lithium acetate, IH: isobutyronitrile.

chain without the initiator terminus (*m/z* 131). When lower collision gas pressures are used, the overall pattern stays the same but the maximum intensity of the distributions are shifted to higher center-of-mass collision energy.

3.2. Molecular modeling

The optimized structures of $[PVAc_5 + Li]^+$ and its fragmentation product ions are shown in Fig. 4 and the relative energies can be found in Table 1. The energy needed for the loss of acetic acid was investigated from the five different positions on the 5-mer, starting at the hydrogen end with position 1 and finishing at the isobutyronitrile end with position 5 as shown in Scheme 2. The resulting structures were optimized using AM1 and their energies were calculated at the HF/6-31+G(d) level of theory. As shown in Table 2, the lowest energy product corresponds to the loss of acetic acid closest to the hydrogen end (position 1). This does not

Table 2
Calculated relative energies for the fragment 5-mer-1AcH

Structure	Position of AcH loss	Relative energies (kJ/mol)[a] HF/6-31+G(d)//AM1
[5-mer-1AcH] + 1AcH	1	21.9
[5-mer-1AcH] + 1AcH	2	55.4
[5-mer-1AcH] + 1AcH	3	29.9
[5-mer-1AcH] + 1AcH	4	25.1
[5-mer-1AcH] + 1AcH	5	47.0

[a] The energies are relative to the 5-mer.

Table 1
Calculated relative energies for MM/MD, AM1 and B3-LYP structures of the decomposition products of poly(vinyl acetate) ionized with lithium

Species	*m/z*	Relative energies (kJ/mol)							
		MM/MD structures			AM1 structures			B3-LYP/3-21G	
		MM/MD	HF/6-31+G(d)	B3LYP/6-31+G(d)	AM1	HF/6-31+G(d)	B3LYP/3-31+G(d)	B3LYP/6-21G	B3LYP/6-31+G(d)
$[5\text{-mer} + Li]^+$	506	0	0	0	0	0	0	0	0
$[5\text{-mer} + Li\text{-}1AcH]^+ + 1AcH$	446	57	49	52	189	18	39	155	22
$[5\text{-mer} + Li\text{-}2AcH]^+ + 2AcH$	386	162	150	132	95	86	90	304	106
$[5\text{-mer} + Li\text{-}2AcH]^+ + 3AcH$	326	274	217	194	123	146	143	546	188
$[5\text{-mer} + Li\text{-}2Ac]^+ + 4AcH$	266	391	324	288	141	179	165	636	205
$[5\text{-mer} + Li\text{-}2AcH\text{-}1\text{-}AcLi]^+ + 3AcH + 1AcLi$	260	−148	747	661	345	286	261	726	290
$[5\text{-mer} + Li\text{-}5AcH]^+ + 5AcH$	206	463	474	428	162	258	240	877	332
$[5\text{-mer} + Li\text{-}4AcH\text{-}1AcLi]^+ + 4AcH + 1AcLi$	200	−231	857	708	329	248	237	828	301
$[Polyene]^+ + 4AcH + 1AcLi + IH$	131	−70	980	794	459	389	358	955	405

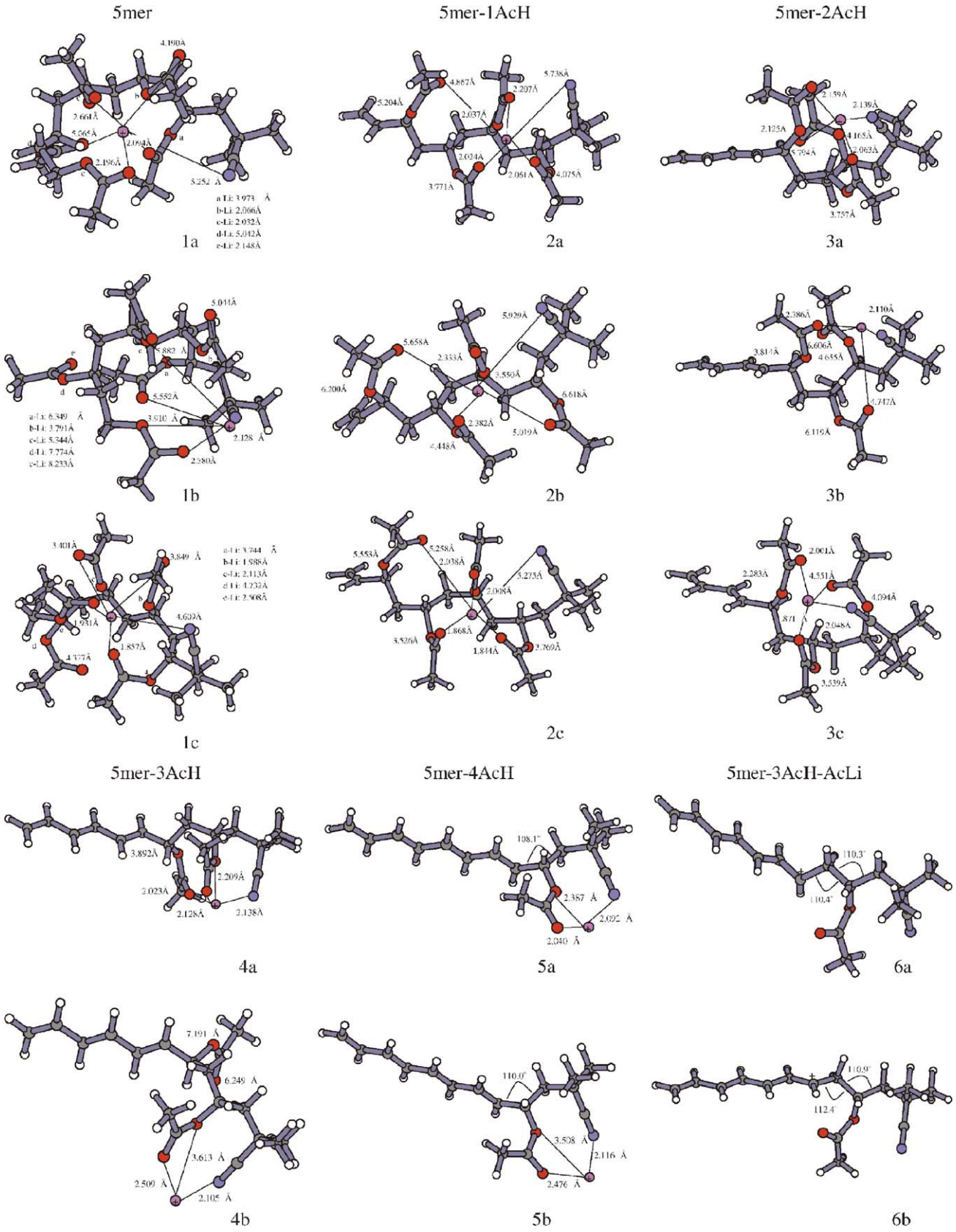

Fig. 4. The optimized structures of $[PVAc_5 + Li]^+$ and its fragments from (a) MM/MD, (b) AM1 and (c) B3-LYP/3-21G optimization. Lithium atoms are labeled with a "+" on the atom. Carbon atoms with a positive charge have a "+" beside them.

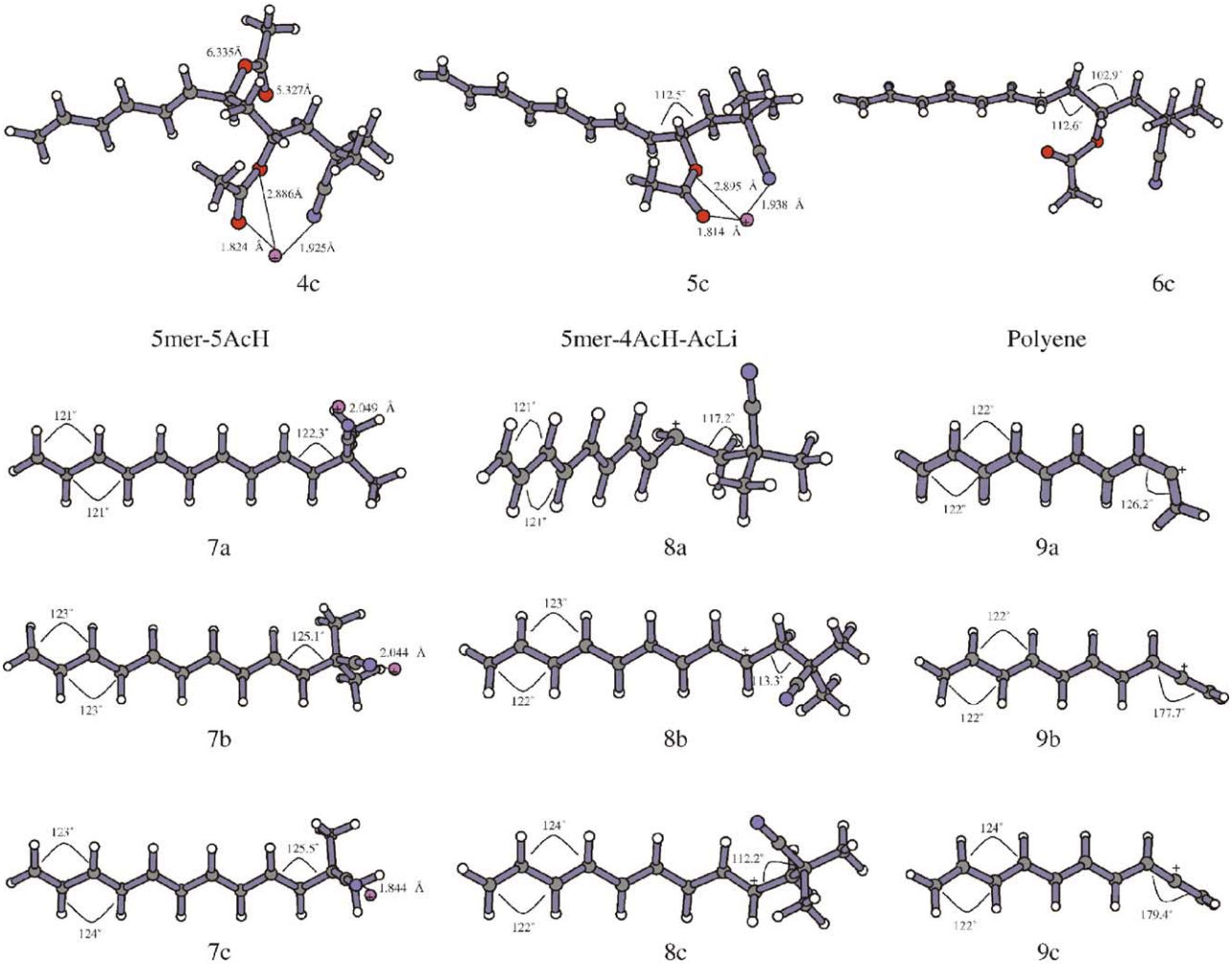

Fig. 4. (*Continued*).

preclude the loss from the other positions, especially since the transition state energies for these processes are like to be similar. The sequential loss of acetic acid should occur from neighboring positions since the product ion will benefit from a conjugated double bond structure. For all the fragments discussed in Table 1, the losses were assumed to start at position 1.

It is clear from Table 1 that the relative energies of the fragments obtained from MM/MD are unreliable as might be expected from the molecular mechanics treatment of gas-phase ions. In addition, MM/MD alone does not provide reliable geometries for further single-point energy calculations. The relative energies for the reactions involving a loss of lithium acetate are particularly poorly represented at this level of theory of geometry optimization. The relative energies using AM1 geometries with HF/6-31+G(d) and B3-LYP/6-31+G(d) single-point energy calculations are slightly lower than the AM1 energies. The relative energies using B3-LYP/3-21G geometries and energies are higher than the AM1 relative energies but the B3-LYP/6-31+G(d)//B3-LYP/3-21G values are closer to the AM1 results. The B3-LYP/6-31+G(d)//B3-LYP/3-21G values are believed to be most reliable results but the AM1 results still present an interest because of the lower calculation time required.

The gas-phase conformation of ionized poly(vinyl acetate) is similar to that of PMMA with the side chains of the polymer coordinating to the metal ion. When the 5-mer ion was optimized by MM/MD, all 10 oxygen atoms and the nitrogen atom of the initiator end group coordinate the Li^+ ion. The distance between the oxygen atoms and the Li^+ range from 2.03 to 5.07 Å. When the structure is optimized by AM1, the Li^+ moves above the molecule, and only four oxygen atoms are less then 5.07 Å from Li^+. The nitrogen atom on the initiator-terminal is now closer to the metal ion (2.12 compared to 5.25 Å at MM/MD). The B3-LYP structure shows the shortest distances between the lithium cation and the oxygen atoms (1.86–4.73 Å).

The structure for 5-mer-AcH, *m/z* 446, exhibits the Li^+ moving away from the double bond, but also further from the nitrogen atom of the initiator end group. For the AM1 structure, the oxygen atoms are generally further from the

Li^+ ion compared to the MM and DFT structures. Unlike structure **2a** and **2c** from Fig. 4, the oxygen atoms on the side chain adjacent to the isobutyronitrile end group in Fig. 2B are far from the metal ion. The structures and trends are similar for the fragment at *m*/*z* 386, corresponding to the loss of two terminal acetic acid molecules.

For the fragment at *m*/*z* 326 (loss of three terminal acetic acid molecules), there is more rigidity limiting the coordination of the salt for the DFT and AM1 structures compared to the MM/MD structure. Only one side chain acetate group and the nitrogen atom stabilize the cation since the oxygen atoms of the other side chain are more then 5.3 Å from the cation. The structures for the fragment at *m*/*z* 266, corresponding to the loss of four acetic acid molecules are similar to those of *m*/*z* 326. In the fragment ion at *m*/*z* 206, corresponding to the loss of five acetic acid molecules, only the nitrogen of the isobutyronitrile remains to complex the Li^+ ion. The structures from the three levels of theory are almost identical except for the orientation of the isobutyronitrile terminal in structure **7a** and the slightly smaller distance between the nitrogen and the Li^+ in the DFT structure **7c**.

The fragments at *m*/*z* 260 and 200 (loss of three or four acetic acid molecules and one lithium acetate moiety) are less planar in the MM/MD optimization compare to the AM1 and DFT optimizations. According to the bond angle, the carbocation of the polyene fragment (*m*/*z* 131) has a sp^2 character when optimized by MM/MD and sp character when AM1 or B3-LYP is used.

3.3. Internal energy and competing fragmentation process

The potential energy surface (PES) in Fig. 5 shows the relative energies obtained at the B3-LYP/6-31+G(d)//B3-LYP/3-21G level of theory. The average internal energy of the 5-mer ion (calculated using the B3-LYP/3-21G vibrational frequencies) at 298 K is 100 kJ/mol. The PES shows irregular steps of either 20 or 100 kJ/mol for the losses of acetic acid molecules. According to the relative energy diagram, the reaction leading to the loss of a fourth acetic acid molecule was significantly lower in energy than the reaction leading to the loss of lithium acetate. This is consistent with the CID mass spectra in which *m*/*z* 266 always predominates over *m*/*z* 260. However, once only a single acetic acid remains on the polymer, it is preferentially lost as a metal acetate (Figs. 2 and 5). The polyene ion (*m*/*z* 131) is the highest energy channel on the surface.

There is a high activation energy required for the 1,5-H rearrangement resulting in the loss of acetic acid. The 1,5-hydrogen rearrangement is known to require up to 175–200 kJ/mol in pyrolysis experiments [19,20]. It is also known that the stability of the resulting ene product affects the barrier height in these reactions. As the polymer loses acetic acid, a conjugated polyene structure is obtained that may successively lower the transition state to acetic acid loss. The transition state for acetic acid loss was modeled for the potential energy surface of a 3-mer with hydrogen atoms at both ends. The geometries of the 3-mer and the transition states were optimized at the HF/6-31+G(d) level of theory since it was considered unlikely that the smaller 3-21G basis set would yield a reliable transition state structure. For acetic acid loss, the minimum energy reaction pathway from a 3-mer-1AcH + Li^+ to a 3-mer-2AcH + Li^+ is shown in Fig. 6 and the structures are presented in Fig. 7. The mechanism consists of the 1,5-H shift to produce an intermediate complex between 3-mer-2AcH and acetic acid bound together by Li^+. The transition state has the Li^+ ion complexing both acetate side chains while the hydrogen

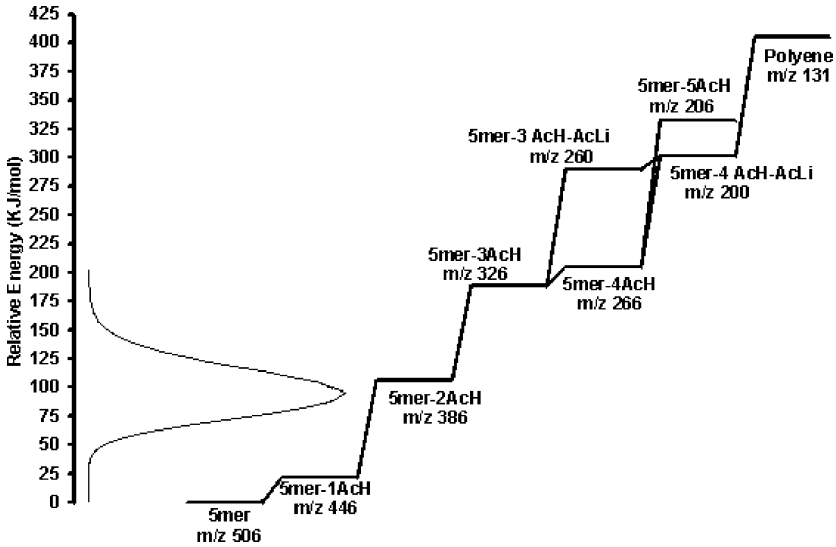

Fig. 5. Relative energy surface for the decomposition of poly(vinyl acetate) ionized with lithium using the B3-LYP/6-31+G(d)//B3-LYP/3-21G level of theory. The thermal energy distribution of the precursor ions at 298 K is superimposed on the diagram. AcH: acetic acid, AcLi: lithium acetate, IH: isobutyronitrile.

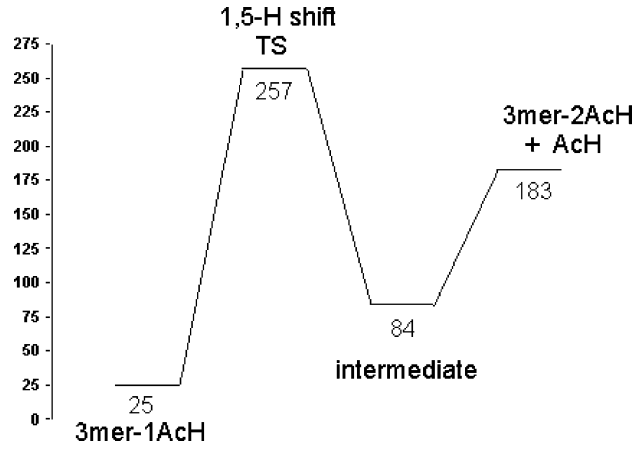

Fig. 6. Potential energy surfaces for the 1,5-H shift leading to acetic acid loss (all energies relative to the 3-mer + Li^+ ion having two hydrogen atom end groups).

atom is transferred. The forward barrier to this process is 232 kJ/mol at this level of theory.

The early appearance of *m*/*z* 200 and *m*/*z* 131 in the CID mass spectra can be explained by the internal energy content of the PVAc ions. The average thermal vibrational energy of the PVAc 5-mer is 100 kJ/mol and the distribution is shown superimposed on the relative energy diagram in Fig. 5. Meroueh and Hase [21,22] and Laskin and Futrell [23] have modeled the internal energy deposition in low energy collision-induced dissociation experiments. For a single 5 eV center-of-mass (cm) collision event, the internal energy deposition ranges from 0 to 5 eV with a maximum at ~0.5 eV. As the number of collisions increases, so does the most probable internal energy deposition [22]. In the present experiments, cm collision energies between 0.3 and 2.8 eV were studied (Fig. 3). At 1 eV, up to 100 kJ/mol can be deposited into the ion which, together with the average thermal internal energy of 100 kJ/mol, is insufficient to raise the internal energy of a large fraction of the ion population above the threshold for polyene ion formation. Multiple collisions must therefore be responsible, but it must be noted that the overall trends in Fig. 3 were independent of collision gas pressure.

Another explanation may be in the "sudden death" approximation in chemical kinetics [24,25]. Laskin and co-workers have observed and modeled the shattering of peptide ions in collision-induced dissociation experiments involving surfaces. This approximation assumes that the energy deposited into the projectile ion is not statistically randomized among the internal modes (rotations and vibrations) of the ion, but rather is localized leading to dissociation channels that would otherwise be inaccessible.

The loss of a dimer of acetic acid was also considered but the resulting relative energies do not correspond to the mass spectrometry results (Table 3). If acetic acid is lost as a dimer, it might be expected that the CID mass spectra would exhibit stronger peaks due to these process, but this is not observed. Indeed, the reaction for loss of one acetic acid molecule is higher in energy than for the loss of a dimer, but the mass spectra in Fig. 2 show a larger abundance for VAc-1AcH. The same pattern is observed for VAc-$(AcH)_2$-1AcH and VAc-2$(AcH)_2$.

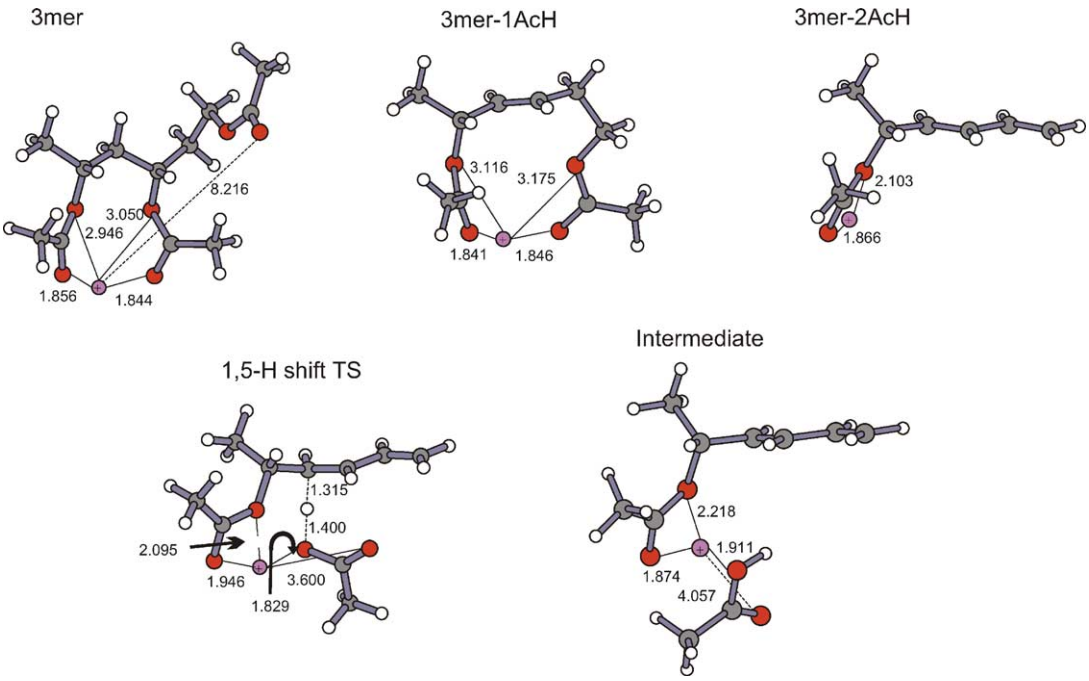

Fig. 7. Optimized HF/6-31+G(d) structures for the 1,5-hydrogen shift transition state for the reaction leading from a 3-mer-1AcH to a 3-mer-2AcH. Bond lengths are given in Angstroms.

Table 3
Calculated relative energies considering the loss of the acetic acid dimer

Structure	Mass (Da)	Relative energies (kJ/mol) B3-LYP/6-31 +G(d)//B3-LYP/3-21G
5-mer	506	0
[5-mer-AcH] + AcH	446	22
[5-mer-AcH_2] + AcH_2	386	3
[5-mer-AcH-AcH_2] + AcH + AcH_2	326	86
[5-mer-2AcH_2] + 2AcH_2	266	−1
[5-mer-AcH-AcH_2-AcLi] + AcH + AcH_2 + AcLi	260	187
[5-mer-AcH-2AcH_2] + AcH + 2AcH_2	206	127
[5-mer-2AcH_2-1AcLi] + 2AcH_2 + AcLi	200	199
[Polyene] + 2AcH_2 + AcLi + IH	131	200

4. Conclusion

Electrospray-ionization tandem mass spectrometry was used to explore the dissociation characteristics of ionized poly(vinyl acetate). Collision-induced dissociation mass spectra showed them to fragment by the sequential loss of acetic acid from the polymer backbone. Molecular mechanics/molecular dynamics was used to find low energy conformations for a 5-mer along with the fragmentation products. This was followed by AM1 and B3-LYP/3-21G level optimizations of these structures and HF/6-31+G(d) and B3-LYP/6-31+G(d) single-point energy calculations to obtain reliable relative energies for each channel. The mass spectra can be understood in terms of the relative product energies, the transition states for 1,5-hydrogen rearrangements, and the internal energy content of the PVAc ions.

Acknowledgements

P.M.M. thanks the Natural Sciences and Engineering Research Council of Canada for financial support as well as Dr. Marc Dubé for his collaboration in the polymer synthesis and the donation of the JAVA™-based program used for simulation of free-radical polymerization. The authors thank Dr. Julia Laskin (Pacific Northwest National Laboratories) for valuable discussions.

References

[1] A.T. Jackson, K.R. Jennings, J.H. Scrivens, J. Am. Soc. Mass Spectrom. 8 (1997) 76.
[2] A.T. Jackson, H.T. Yates, J.H. Scrivens, M.R. Green, R.H. Bateman, J. Am. Soc. Mass Spectrom. 8 (1997) 1206.
[3] J.H. Scrivens, A.T. Jackson, H.T. Yates, M.R. Green, G. Critchley, J. Brown, R.H. Bateman, M.T. Bowers, J. Gidden, Int. J. Mass Spectrom. 165/166 (1997) 363.
[4] A.T. Jackson, H.T. Yates, J.H. Scrivens, G. Critchley, J. Brown, M.R. Green, R.H. Bateman, Rapid Commun. Mass Spectrom. 10 (1996) 1668.
[5] J. Gidden, A.T. Jackson, J.H. Scrivens, M.T. Bowers, Int. J. Mass Spectrom. 188 (1999) 121.
[6] M.J. Deery, K.R. Jennings, C.B. Jasieczek, D.M. Haddleton, A.T. Jackson, H.T. Yates, J.H. Scrivens, Rapid Commun. Mass Spectrom. 11 (1997) 57.
[7] A.T. Jackson, H.T. Yates, J.H. Scrivens, M.R. Green, R.H. Bateman, J. Am. Soc. Mass Spectrom. 9 (1998) 269.
[8] A.T. Jackson, A. Bunn, L.R. Hutchings, F.T. Kiff, R.W. Richards, J. Williams, M.R. Green, R.H. Bateman, Polymer 41 (2000) 7437.
[9] J. Gidden, M.T. Bowers, A.T. Jackson, J.H. Scrivens, J. Am. Soc. Mass Spectrom. 13 (2002) 499.
[10] Z. Jedlinski, G. Adamus, M. Kowalczul, R. Schubert, Z. Szewczuk, P. Stefanowicz, Rapid Commun. Mass Spectrom. 12 (1998) 357.
[11] R. Chen, A.M. Tseng, M. Ushing, L. Li, J. Am. Soc. Mass Spectrom. 12 (2001) 55.
[12] T.L. Selby, C. Wesdemiotis, R.P. Lattimer, J. Am. Soc. Mass Spectrom. 5 (1994) 1081.
[13] A.R. Bottrill, A.E. Giannakopulos, C. Waterson, D.M. Haddleton, K.S. Lee, P.J. Derrick, Anal. Chem. 71 (1999) 3637.
[14] J. Gidden, T. Wyttenbach, A.T. Jackson, J.H. Scrivens, M.J. Bowers, J. Am. Chem. Soc. 122 (2000) 4692.
[15] C. Badeen, M.A. Dubé, Polym. React. Eng. 11 (2003) 53.
[16] Molecular Simulations Inc., Cerius2 Modeling Environment, Molecular Simulations Inc., San Diego, 1999.
[17] M.J. Frisch, G.W. Trucks, H.B. Schlegel, G.E. Scuseria, M.A. Robb, J.R. Cheeseman, V.G. Zakrzewski, J. J.A. Montgomery, R.E. Stratmann, J.C. Burant, S. Dapprich, J.M. Millam, A.D. Daniels, K.N. Kudin, M.C. Strain, O. Farkas, J. Tomasi, V. Barone, M. Cossi, R. Cammi, B. Mennucci, C. Pomelli, C. Adamo, S. Clifford, J. Ochterski, G.A. Petersson, P.Y. Ayala, Q. Cui, K. Morokuma, D.K. Malick, A.D. Rabuck, K. Raghavachari, J.B. Foresman, J. Cioslowski, J.V. Ortiz, A.G. Baboul, B.B. Stefanov, G. Liu, A. Liashenko, P. Piskorz, I. Komaromi, R. Gomperts, R.L. Martin, D.J. Fox, T. Keith, M.A. Al-Laham, C.Y. Peng, A. Nanayakkara, C. Gonzalez, M. Challacombe, P.M.W. Gill, B. Johnson, W. Chen, M.W. Wong, J.L. Andres, C. Gonzalez, M. Head-Gordon, E.S. Replogle, J.A. Pople, GAUSSIAN 98 RevA.7. Gaussian Inc., 1998.
[18] A.P. Scott, L. Radom, J. Phys. Chem. 100 (1996) 16502.
[19] M.C. Lin, K.J. Laidler, Trans. Faraday Soc. 64 (1968) 927.
[20] G.M. Wieder, R.A. Marcus, J. Chem. Phys. 37 (1962) 1835.
[21] O. Meroueh, W.L. Hase, J. Phys. Chem. A 103 (1999) 3981.
[22] O. Meroueh, W.L. Hase, Int. J. Mass Spectrom. 201 (2000) 233.
[23] J. Laskin, J.H. Futrell, J. Chem. Phys. 116 (2002) 4302.
[24] J. Laskin, T.H. Bailey, J.H. Futrell, J. Am. Chem. Soc. 125 (2003) 1625.
[25] S.O. Meroueh, Y. Wang, W.L. Hase, J. Phys. Chem. A 106 (2002) 9983.